Capturing the Scale Dependency of Erosion-Induced Variation in CO_2 Emissions on Terraced Slopes

Yaxian Hu[1]*, Vincent Schneider[2], Brigitte Kuhn[2], Shengli Guo[1] and Nikolaus J. Kuhn[2]

[1]State Key Lab of Soil Erosion and Dryland Farming on the Loess Plateau, Institute of Soil and Water Conservation, Northwest A&F University, Yangling, China, [2]Physical Geography and Environmental Change, Department of Environmental Sciences, University of Basel, Basel, Switzerland

Net soil CO_2 emissions are not independent of topography but tend to decline with increasing slope gradients. Such decline has been attributed to increased runoff and greater soil loss on steep slopes, leaving the soil less habitable for microorganisms. However, the specific variations of slope gradients and thus the associated soil properties relevant for CO_2 emissions, especially from terraced slopes, are often disguised by the coarse resolution of digital terrain models (DTMs) based on commonly available open-source data. Such misrepresentation of the relationship between topography and soil CO_2 emissions carries the risk of a wrong assessment of soil-atmosphere interaction. By applying a slope dependent soil CO_2 emission model developed from erosion plots to nearby sloping and partially terraced cropland using two DTMs of different spatial resolutions, this study tested the significance of these resolution-induced errors on CO_2 emission estimates. The results show that the coarser-resolution Shuttle Radar Topography Mission (SRTM) underestimated CO_2-C emission by 27% compared to the higher-resolution DTM derived from Unmanned Aerial Vehicles (UAV) imagery. Such difference can be mostly attributed to a better representation of the proportion of flat slopes in the high-resolution DTM. Although the observations from erosion plots cannot be directly extrapolated to a larger scale, the 27% underestimation using the coarser-resolution SRTM DTM emphasizes that it is essential to represent microreliefs and their impact on runoff and erosion-induced soil heterogeneity at an appropriate scale. The widespread impact of topography on erosion and deposition on cropland, and the associated slope-dependent heterogeneity of soil properties, may lead to even greater differences than those observed in this study. The greatly improved estimation on CO_2 emissions by the UAV-derived DTM also demonstrates that UAVs have a great potential to fill the gap between conventional field investigations and commonly applied coarse-resolution remote sensing when assessing the impact of soil erosion on global soil-atmosphere interaction.

Keywords: slope gradient, soil CO_2 emissions, soil erosion, digital terrain model, terraced field

INTRODUCTION

A substantial number of studies have utilized a combination of field data and remote sensing to assess the potential impacts of soil erosion on atmospheric CO$_2$ at various spatiotemporal scales (Nadeu et al., 2012; Yue et al., 2016; Borrelli et al., 2017; Wilken et al., 2017; Lugato et al., 2018). One of the common complications in this research is the compatibility between the resolution of digital terrain models (DTMs) and the field topographic features and processes to be represented (Lu et al., 2020). Presumably, large scale topographic maps (e.g., 1:10,000) can produce DTMs of more desirable accuracy, but highly accurate topographic data is not always available, processable by available computers, or is often too expensive to be acquired. Yet, freely accessible data sources with lower resolutions often bear great uncertainties when assessing slope-scale soil erosion risk and impacts. The rates of erosion by water and gravity, including tillage and intentional soil redistribution, are all slope-dependent and much more sensitive to minor topographic variations than a coarse resolution grid cell DTM would reflect (Kirkby, 2010; Balaguer-Puig et al., 2018; He et al., 2020). This in turn introduces potentially significant uncertainties when accounting for erosion-induced spatial redistribution of soil water and nutrients (Li et al., 2018), and hence the vertical CO$_2$ exchanges with the atmosphere in a landscape characterized by small-scale soil redistribution (Du et al., 2020b).

Previous studies have demonstrated that slope-induced erosion can potentially affect the spatial distribution of soil water, nutrients and microbial communities (Du et al., 2020a, Du et al., 2020b; Hu et al., 2016; Wang et al., 2014, Wang et al., 2017b), which all possibly introduce variations to CO$_2$ emissions from eroded soil (Nitzsche et al., 2017; Hu et al., 2020b). In particular, an exponentially declining pattern of soil CO$_2$ emissions was observed when slope gradients increased from 0 to 20°(Hu et al., 2020b), highlighting the potential uncertainty in simulated greenhouse gas contributions from sloped and terraced fields to the atmosphere. Assessing emissions accurately therefore requires an effective DTM to represent slope dependent CO$_2$ emissions in soil-atmosphere models. However, the impact of features such as narrow terraces or short slopes on soil respiration is not captured by raster cells representing hectares to square kilometers in size commonly used in regional or global scale CO$_2$ emission models (Yue et al., 2016; Borrelli et al., 2017; Lugato et al., 2018). Even if those models had a greater spatial resolution, easily available open source topography data, such as the 30 m × 30 m Shuttle Radar Topography Mission (SRTM) data of the US Geological Survey or similar elevation data, do not capture the impact of microreliefs on soil respiration. Laser scanning techniques, such as airborne laser scanning (ALS) or terrestrial laser scanning (TLS), can create high resolution and accurate DTMs, but the heterogeneous point densities, undesired return signals from vegetation, prolonged working hours with multiple scans, and sophisticatedly designed tie points to align orientations of individual scans largely hinder their application to capture microreliefs in rugged landscapes with complex terrains (Baltensweiler et al., 2017; Ou et al., 2021). With fast

development of photogrammetric techniques and increasing accessibility of Unmanned Aerial Vehicles (UAVs) and high-resolution cameras, improved DTMs for a large area, even with complex terrains, can be easily obtained within a short time by stitching highly overlapping images (Schwanghart et al., 2013; Krenz and Kuhn, 2019; Hu et al., 2020a). Hence, this promises great opportunities to accurately assess the scale-dependent variation of CO$_2$ emissions on terraced slopes.

This case study was conducted on a terraced field on the Chinese Loess Plateau (**Figure 1**), where soilscapes have been fragmented intensively by establishing check-dams and terraces (Ostwald and Chen, 2006; Sun et al., 2014; Wang et al., 2017a). The Chinese Loess Plateau thus recommends itself as a suitable area to identify the potential role of a misrepresentation of slope dependent soil redistribution on CO$_2$ emissions. To assess the potential errors for such topographic scale-dependent CO$_2$ emissions on eroding cropland, a simple slope dependent CO$_2$ emission model developed on the same loess soil, was adopted and applied to two DTMs, derived from SRTM and UAV imagery respectively. The aim of this study was to identify the potential errors of CO$_2$ emissions on terraced slopes induced by ignoring microreliefs.
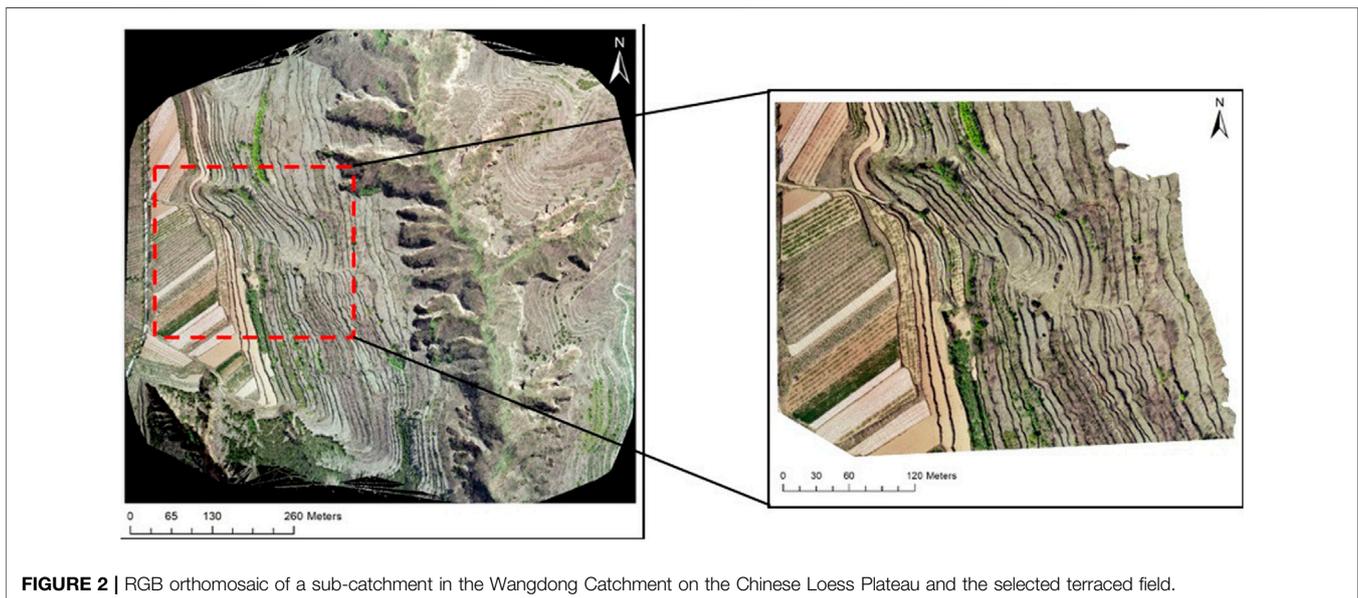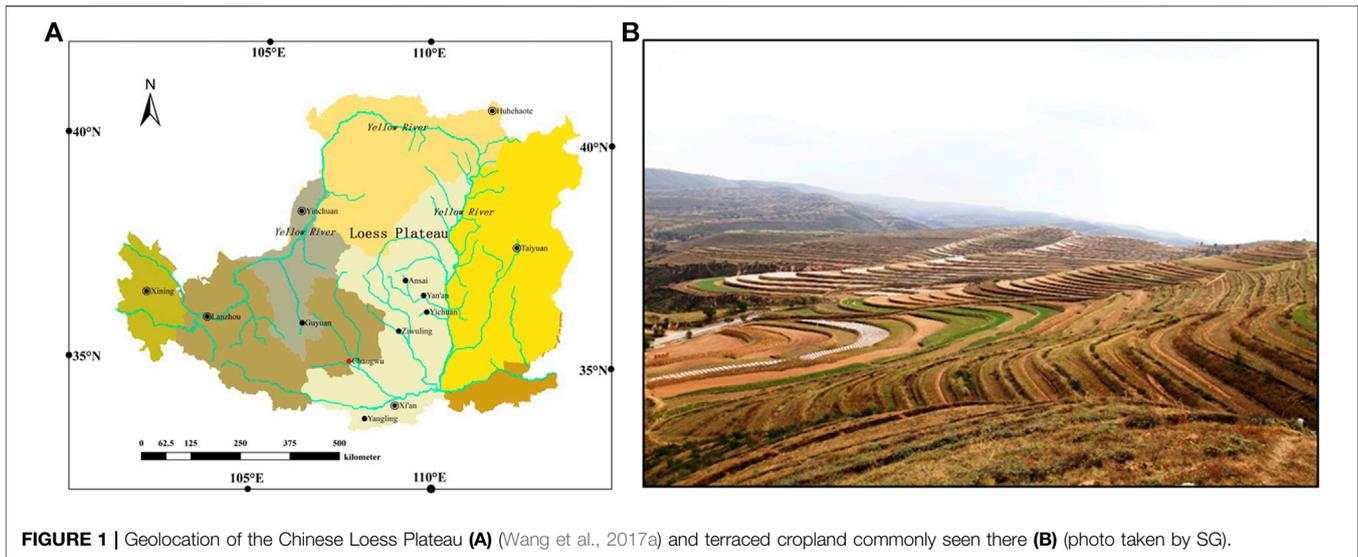
MATERIALS AND METHODS

Study Area
The study area is in the Wangdong Catchment (35°13′N–35°16′N, 107°40′E–107°42′E, average altitude: 1,220 m a.s.l.), southwestern part of the Chinese Loess Plateau. Highly erodible loess soil combined with concentrated rainfall in summer, and further accelerated by intensive cultivation, once made this region one of the most eroded region in the world. In consequence, the plateau had been incised into tableland (fragmented plateau), slopes (or gullies) and deposited sediment in valley bottoms (Wang et al., 2017a). To expand agriculture land, terraces had been established on almost every aspect of all the slopes to increase infiltration (**Figure 1**), which were then converted back to forest, grassland or natural rehabilitation in 1990s to curb soil erosion.

Acquisition of Terrain Models From Shuttle Radar Topography Mission and Unmanned Aerial Vehicle
Two DTMs with different spatial resolutions were applied to the Wangdong catchment that had been remained natural rehabilitation since 1990s, specifically on an east-facing terraced slope (about 0.1 km^2) with uneven heights and widths (**Figure 2**). One DTM was based on the open source SRTM from the US Geological Survey (30 m × 30 m), accessed on June 15th, 2018 with raster projected to WGS 1984 UTM Zone 48N. The other DTM was created based on the Structure from Motion (SfM) photogrammetric technique using the UAV imagery obtained on April 19th, 2018. The slope gradients of the study area were then calculated from the two DTMs with ESRI ArcGIS. The UAV used in this study was a Phantom 3 Professional

FIGURE 1 | Geolocation of the Chinese Loess Plateau **(A)** (Wang et al., 2017a) and terraced cropland commonly seen there **(B)** (photo taken by SG).

FIGURE 2 | RGB orthomosaic of a sub-catchment in the Wangdong Catchment on the Chinese Loess Plateau and the selected terraced field.

quadrocopter with a gimbal manufactured by DJI (SZ DJI Technology Co., Ltd., Shenzhen, China). The camera was DJI FC300X (GoPro Inc, San Mateo, California, United States), with a 1/2.3" 12.4-megapixel CMOS sensor and an exposure time automatically adjusted. Images were taken at an altitude of 100 m above the plateau with an angle of 90° and an average overlap of 80%. Given that the width of terraces on the selected slope range from 3 to 15 m, the ground sampling distance (GSD) of 5.25 cm was considered adequate to reflect the essential features of terraced slopes. Navigation was GPS-based (under coordinate system WGS 1984 UTM Zone 48N) using an image acquisition program of Pix4D Capture App on iPad min A1550. We acknowledged that the resolution of the DTM could be compromised by the changes of altitude along the descending slope. Hence, five ground control points (GCPs) were placed before the arial flight at different altitudes with a "zig-zag" pattern to the furthest point one could manage to descend. The ground coordinates of the GCPs were recorded by a real-time kinematic positioning apparatus (RTK, CHC-i60, Huace, Shanghai, China) coupled with a HCE300 field surveying controller (Huace, Shanghai, China). The coordinates were recorded under China CGCS 2000 by Gaussian Projection. The horizontal accuracy of the RTK system was $\pm (10 + 1 \times 10^{-6} \times distance)$ mm and the vertical accuracy was $\pm (20 + 1 \times 10^{-6} \times distance)$ mm.

All the UAV images were processed using the commercial photogrammetry software Pix4Dmapper Pro (Pix4D SA, Lausanne, Switzerland) and georeferenced according to the GPS positions following the steps listed in Krenz and Kuhn

FIGURE 3 | Slope-dependent CO_2 emission model **(A)** developed from erosion plots **(B)** nearby the Wangdong Catchment, Chinese Loess Plateau. More descriptions on the slope-dependent CO_2 emission model, please refer to Hu et al. (2020b); to learn more about the setting up of erosion plots, please refer to Du et al. (2020a).
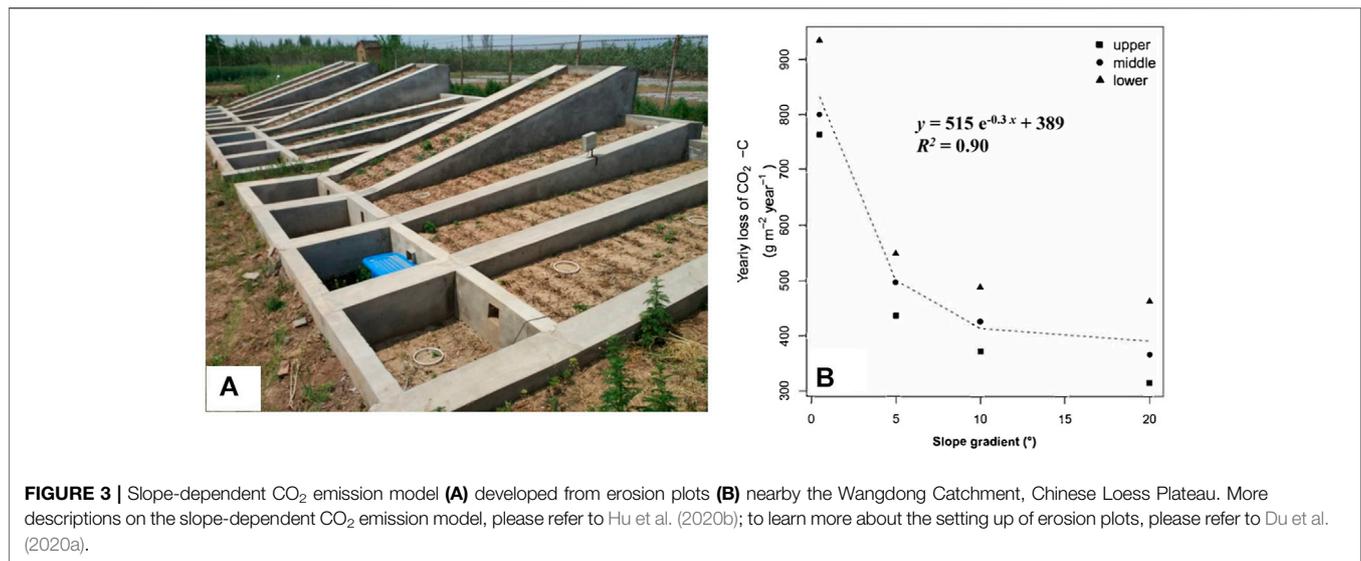
(2019). In brief, after imported into the software, all the images were automatically matched, and bundle-block adjusted. The accurate geolocations of the five GCPs were then added and marked manually on different images to produce a densified point cloud and a 3D textured mesh, which were further used to obtain a DTM (with resolution of 5 × GSD) and a georeferenced orthomosaic. Slope gradient was determined for each pixel of the UAV imagery using QGIS based on the approach developed by Zevenbergen and Thorne (1987). Since the potential influences of vegetation on CO_2 emissions were out of the reach of this study, areas covered by vegetation were identified on the DTM and then excluded from calculation. Areas with a gradient >30° were not covered by soil, and thus were digitized manually from the UAV-based DTM and excluded from the calculations to avoid any overestimation of emissions. The SRTM-DTM did not show any areas with slopes >30°, and consequently, no areas were excluded in agreement with the purpose of this study.

Slope-Dependent Soil CO_2 Emissions

The slope dependent CO_2 emission model (**Eq. 1**) was developed from the year-round observations on four erosion plots with different slope gradients: 0.5°, 5°, 10°, 20° (**Figure 3**). The development of this slope dependent CO_2 emission model has been reported in Hu et al. (2020a). The slope dependent CO_2 emission model reads as:
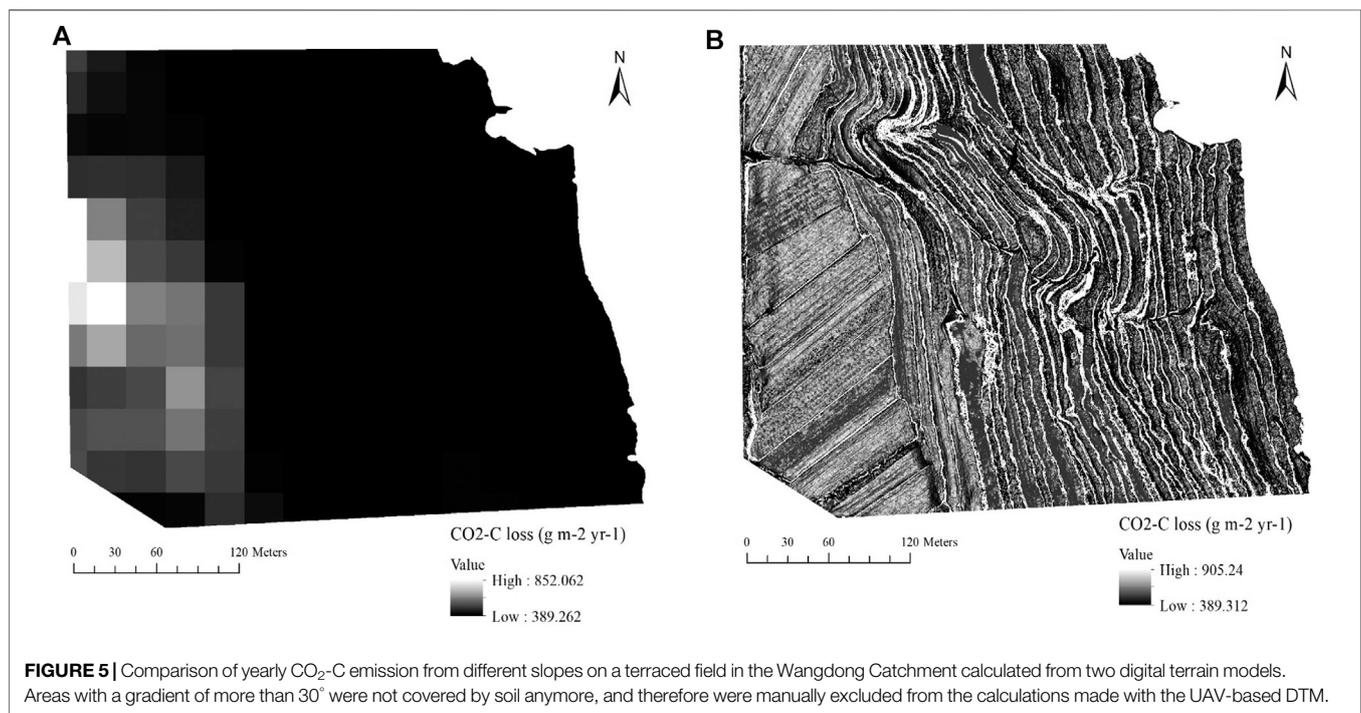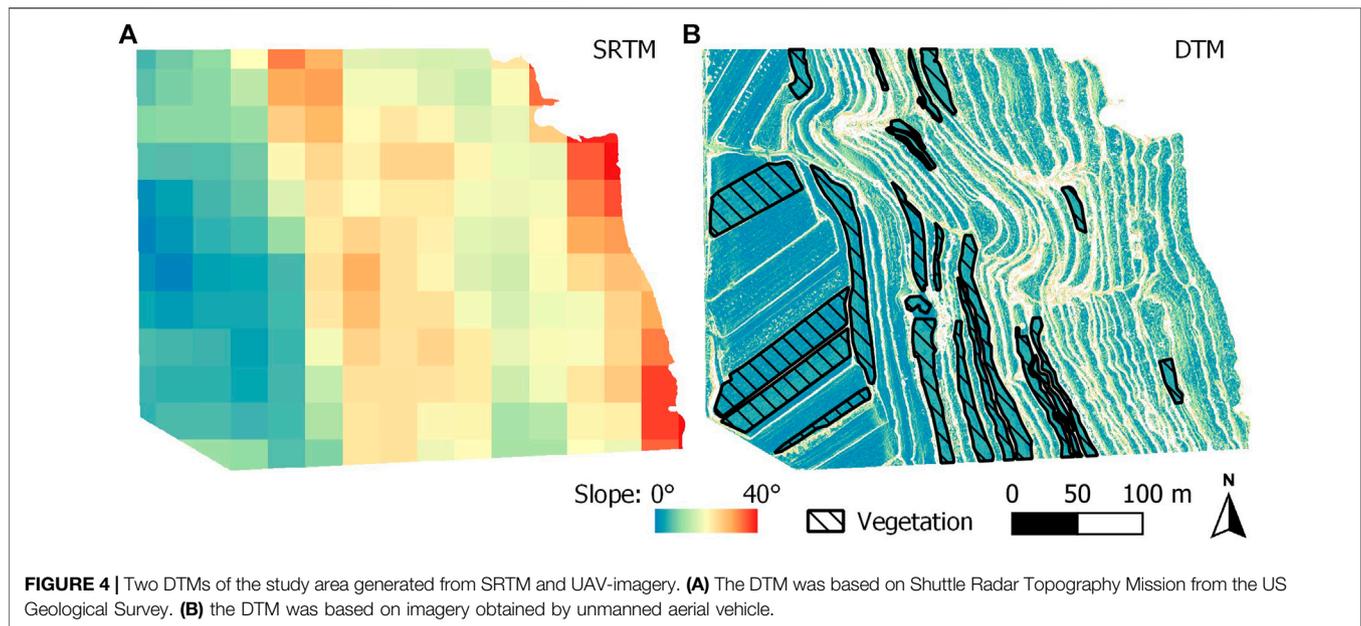
$$y = 515e^{-0.3x} + 389 \qquad (1)$$

where y represents the yearly CO_2-C (g m^{-2} yr^{-1}) at slope gradient of x (°) with an R^2 of 0.90.

The four east-facing erosion plots were established in the nearby Changwu State Key Agro-Ecological Experimental Station by refilling with the same loam soil (Cumulic Haplustoll as in the USDA Soil Taxonomy System) developed from loess deposits as in the terraced fields (Du et al., 2020a). After establishment, the erosion plots were remained uncultivated to simulate the natural rehabilitation as in the terraced fields in the Wangdong

Catchment. Specific descriptions on erosion plots and their setting up have been reported in Du et al. (2020a) (**Figure 3**). In brief, each erosion plot was 5 m × 1 m with three replicates, to represent the common slope gradients on the Loess Plateau (Shen et al., 2016). At the lower end of each erosion plot, there was an outlet channeled into a sediment trap to collect runoff and sediment samples (**Figure 3**). During the experimental year from October 2014 to September 2015, there were in total 534.5 mm precipitation, with five rainfall events that generated detectable runoff and sediment discharge. The runoff and soil net erosion rate reached 4.56 mm and 125.4 g m^{-2}, respectively (Hu et al., 2020b). Although the erosion plots employed in this study were slightly smaller than typical terraces in the study area (3–15 m), previous observations have proved their adequate length and inclination to distinguish the effects slope gradients on soil CO_2 emissions (Wang et al., 2017b; Du et al., 2020a). The soil CO_2 emission rates on each eroding slope were measured every 10 days during the experimental year, following the protocol described in Du et al. (2020a). With the semi-arid climatic conditions and well-drained loess soil, we presumed that the likelihood of carbon emission as methane was low (Brzezińska et al., 2012). Therefore, carbon mineralization through CO_2 emissions was described as CO_2-C in this study to illustrate that our measurements captured only CO_2 emissions without considering other gaseous manners.

RESULTS AND DISCUSSION

In the coarse 30 × 30 m SRTM-derived DTM, only the major geomorphological features such as plateau and slopes were clearly distinguished (**Figure 4**). It did not capture the narrow width of the terraces (3–15 m) and attributes mostly intermediate slope angles to the terraces. The UAV-derived DTM, on the other hand, reflected the terracing on slope length and gradient well, i.e., flat steps separated by retaining walls or naturally steep ravine side-slopes. Applying the CO_2 emission model to the selected terraced

FIGURE 4 | Two DTMs of the study area generated from SRTM and UAV-imagery. **(A)** The DTM was based on Shuttle Radar Topography Mission from the US Geological Survey. **(B)** the DTM was based on imagery obtained by unmanned aerial vehicle.

FIGURE 5 | Comparison of yearly CO$_2$-C emission from different slopes on a terraced field in the Wangdong Catchment calculated from two digital terrain models. Areas with a gradient of more than 30° were not covered by soil anymore, and therefore were manually excluded from the calculations made with the UAV-based DTM.

field generated a CO$_2$-C emission of 392 g m^{-2} yr^{-1} for the SRTM-derived DTM and 451 g m^{-2} yr^{-1} for the high-resolution UAV-derived DTM (**Figure 5**). When weighted by slope gradient distribution in the study area, the difference in CO$_2$-C emission was even greater, generating 537 g m^{-2} yr^{-1} for the UAV-derived DTM and 423 g m^{-2} yr^{-1} for in the SRTM-derived DTM (**Figure 5**).

The differences between the slope dependent CO$_2$-C emission calculated from the two DTMs of the study site clearly

demonstrate an inherent risk associated with ignoring the actual topography. Although the slope-dependent CO$_2$ emissions can vary with pixel size when the UAV-derived DTM was of different resolutions, the difference between the CO$_2$ emission values between SRTM- and UAV-derived DTMs can be considered as indicative of the sensitivity of emission calculations to the spatial patterns of soil along slopes affected by erosion and deposition. We must acknowledge that the comparison of CO$_2$ emissions derived from the two DTMs in

this study is obviously biased by the terraced topography, thus leading to a larger area with intermediate slope gradients and in turn lower emission totals. However, a bi-modal distribution of slope gradient frequency is not uncommon in terraced land (Wei et al., 2016; Chen et al., 2017). Hence, reliable estimation on CO$_2$ emissions must be microrelief-specific, especially when considering that terraced fields constitute at least 10% of the entire cropland area globally (1.1 billion ha, Roser and Ritchie, 2019) and distribute widely in almost all the major grain producing regions. For instance, 22 million ha in Middle east and North Africa (Dixon et al., 2001), 13 million ha in China (Chapagain and Raizada, 2017), 133 million ha rice field in Asian-Pacific region that is often terraced (Papademetriou, 2000), as well as smaller areas such as vineyards in Europe and South America (Chapagain and Raizada, 2017; Varotto et al., 2019).

In more general terms, the greater emissions from the UAV-derived DTM illustrate that when the raster cells in DTMs were greater than the actual topographic features, it would potentially lead to significant errors of agricultural land CO$_2$ emissions. Such errors are dependent on how close the pixel size is to the microreliefs and would thus be particularly pronounced in landscapes with short slopes and contrasting erosion and deposition-induced soil development along them (e.g., Van Oost et al., 2009; Greenwood et al., 2015; Hu et al., 2016; Lu et al., 2020). However, such discrepancy induced by using improper pixel size to model slope dependent impacts on surface processes or biogeochemistry is not uncommon in recent global and regional-scale studies addressing erosion and climate change (e.g., 250 m × 250 m in Borrelli et al., 2017; 1 km × 1 km in Lugato et al., 2018). They would be too coarse to capture the potential impacts of finer scale topographic features on runoff, erosion and deposition, and thus soil respiration. Soil disturbance introduced by human activities, such as establishing terraces, conducting tillage and land leveling practices, or planting different vegetations, can also introduce spatial and temporal variations in slope-dependent CO$_2$ emissions (Gao et al., 2020; Li et al., 2020), further highlighting the essence to create DTMs with proper pixel size and resolution in assessing regional carbon balance.

Overall, the slope dependency of CO$_2$ emissions in this study is a showbox exhibiting the decisive role of the DEM resolution and pixel size in calculating regional carbon balance. Certainly, the flight protocol and resolution of DTM employed in this study cannot be directly applied to estimate CO$_2$ emissions from other regions with local reliefs, different soil properties and land use types. A sensitivity study with different resolutions of UAV-derived DTM is essential to understand at which pixel size occurs the most significant variations in the slope dependent CO$_2$ emissions. The greatly improved estimation of CO$_2$ emissions by the UAV-derived DTM further demonstrates that UAVs with high spatial resolution have a great potential to fill the gap between conventional field investigation and commonly applied coarse-resolution remote sensing for assessing the impact of soil erosion on soil respiration. While the resolution of global DTMs might still not capture microreliefs relevant for erosion, combining UAV-derived DTMs with soil biogeochemical data could be used to enable the development of parameters that capture the influence of topography on soil-atmosphere interaction at a landscape scale. Moreover, sequential UAV investigations at decadal intervals also promise a good opportunity to enable stakeholders to evaluate the flattening of deserted terraces evolved over repeated erosion processes, and the thus induced variations in regional carbon balances.

CONCLUSION

This study applied a slope-dependent CO$_2$ emission model to calculate yearly carbon emissions from a partially terraced study site on the Loess Plateau, with the aim to identify possible errors introduced by DTMs of different spatial resolutions. After weighted according to slope gradient, the estimated CO$_2$-C emission was 27% greater for a high-resolution DTM than for the coarse-resolution SRTM-based DTM. The difference was attributed to the overestimation of slope steepness in the SRTM-based DTM and associated lower respiration rates. While this difference is biased by the terraced slope we selected for this study, our results still highlight that soil CO$_2$ emissions were sensitive to small topographic features. This indicates that topography and associated surface processes such as erosion and deposition, and soil properties on sloping land, must be represented on a scale that is adequate to capture soil-atmosphere carbon fluxes in global-scale biogeochemical models. The use of UAVs offers the possibility to create topographic data with high spatial resolution, filling the gap between conventional field investigation and commonly applied coarse-resolution remote sensing for assessing the impact of erosion on soil respiration.

DATA AVAILABILITY STATEMENT

The original contributions presented in the study are included in the article/Supplementary Material, further inquiries can be directed to the corresponding author.

AUTHOR CONTRIBUTIONS

YH assisted the field investigation with the UAV, analyzed the slope-dependent CO$_2$ model and wrote the manuscript; VS processed the UAV data and SRTM data; BK conducted the UVA flight in the field and supervised VS for data processing; SG offered local geo-and climate-information and field facilities; NK conceived the concept and structured the manuscript.

FUNDING

REFERENCES

Balaguer-Puig, M., Marqués-Mateu, Á., Lerma, J. L., and Ibáñez-Asensio, S. (2018). Quantifying Small-Magnitude Soil Erosion: Geomorphic Change Detection at Plot Scale. *Land Degrad. Develop.* 29, 825–834. doi:10.1002/ldr.2826

Baltensweiler, A., Walthert, L., Ginzler, C., Sutter, F., Purves, R. S., and Hanewinkel, M. (2017). Terrestrial Laser Scanning Improves Digital Elevation Models and Topsoil pH Modelling in Regions with Complex Topography and Dense Vegetation. *Environ. Model. Softw.* 95, 13–21. doi:10.1016/j.envsoft.2017.05.009

Borrelli, P., Robinson, D. A., Fleischer, L. R., Lugato, E., Ballabio, C., Alewell, C., et al. (2017). An Assessment of the Global Impact of 21st century Land Use Change on Soil Erosion. *Nat. Commun.* 8, 1–13. doi:10.1038/s41467-017-02142-7

Brzezińska, M., Nosalewicz, M., Pasztelan, M., and Włodarczyk, T. (2012). Methane Production and Consumption in Loess Soil at Different Slope Position. *Scientific World J.* 2012, 620270. doi:10.1100/2012/620270

Chapagain, T., and Raizada, M. N. (2017). Agronomic Challenges and Opportunities for Smallholder Terrace Agriculture in Developing Countries. *Front. Plant Sci.* 8. doi:10.3389/fpls.2017.00331

Chen, D., Wei, W., and Chen, L. (2017). Effects of Terracing Practices on Water Erosion Control in China: A Meta-Analysis. *Earth-Science Rev.* 173, 109–121. doi:10.1016/j.earscirev.2017.08.007

Dixon, J., Gulliver, A., Gibbon, D., and Hall, M. (2001). *Farming Systems and Poverty: IMPROVING FARMERS' LIVELIHOODS IN A CHANGING WORLD.* Rome, Italy: FAO.

Du, L., Wang, R., Gao, X., Hu, Y., and Guo, S. (2020a). Divergent Responses of Soil Bacterial Communities in Erosion-Deposition Plots on the Loess Plateau. *Geoderma* 358, 113995. doi:10.1016/j.geoderma.2019.113995

Du, L., Wang, R., Hu, Y., Li, X., Gao, S., Wu, X., et al. (2020b). Contrasting Responses of Soil C-Acquiring Enzyme Activities to Soil Erosion and Deposition. *CATENA* 198, 105047. doi:10.1016/j.catena.2020.105047

Gao, X., Li, W., Salman, A., Wang, R., Du, L., Yao, L., et al. (2020). Impact of Topsoil Removal on Soil CO2 Emission and Temperature Sensitivity in Chinese Loess Plateau. *Sci. Total Environ.* 708, 135102. doi:10.1016/j.scitotenv.2019.135102

Greenwood, P., Kuonen, S., Fister, W., and Kuhn, N. J. (2015). The Influence of Terracettes on the Surface Hydrology of Steep-Sloping and Subalpine Environments: Some Preliminary Findings. *Geogr. Helv.* 70, 63–73. doi:10.5194/gh-70-63-2015

He, Y., Hu, Y., Gao, X., Wang, R., Guo, S., and Li, X. (2020). Minor Topography Governing Erosional Distribution of SOC and Temperature Sensitivity of CO₂ Emissions: Comparisons between Concave and Convex Toposequence. *J. Soils Sediments* 20, 1906–1919. doi:10.1007/s11368-020-02575-6

Hu, Y., Berhe, A. A., Fogel, M. L., Heckrath, G. J., and Kuhn, N. J. (2016). Transport-distance Specific SOC Distribution: Does it Skew Erosion Induced C Fluxes?. *Biogeochemistry* 128, 339–351. doi:10.1007/s10533-016-0211-y

Hu, Y., Fister, W., He, Y., and Kuhn, N. J. (2020a). Assessment of Crusting Effects on Interrill Erosion by Laser Scanning. *PeerJ* 8, e8487. doi:10.7717/peerj.8487

Hu, Y., Wang, Z., Wang, R., Yao, L., and Guo, S. (2020b). Slope Sensitivity: A Coefficient to Represent the Dependency of Soil CO2 Emissions to Slope Gradients. *CATENA* 193, 104659. doi:10.1016/j.catena.2020.104659

Kirkby, M. J. (2010). Distance, Time and Scale in Soil Erosion Processes. *Earth Surf. Process. Landforms* 35, 1621–1623. doi:10.1002/esp.2063

Krenz, J., and Kuhn, N. J. (2019). "Assessing Badland Sediment Sources Using Unmanned Aerial Vehicles," in *Badland Dynamics in the Context of Global Chnage.* Editors E. Nadal-Romero, J. F. Martínez-Murillo, and N. J. Kuhn (Elsevier), Chapter 8, 255–276.

Li, W., Gao, X., Wang, R., Du, L., Hou, F., He, Y., et al. (2020). Soil Redistribution Reduces Integrated C Sequestration in Soil-Plant Ecosystems: Evidence from a Five-Year Topsoil Removal and Addition experiment. *Geoderma* 377, 114593. doi:10.1016/j.geoderma.2020.114593

Li, X., McCarty, G. W., Karlen, D. L., and Cambardella, C. A. (2018). Topographic Metric Predictions of Soil Redistribution and Organic Carbon in Iowa Cropland fields. *Catena* 160, 222–232. doi:10.1016/j.catena.2017.09.026

Lu, S., Liu, B., Hu, Y., Fu, S., Cao, Q., Shi, Y., et al. (2020). Soil Erosion Topographic Factor (LS): Accuracy Calculated from Different Data Sources. *Catena* 187, 104334. doi:10.1016/j.catena.2019.104334

Lugato, E., Smith, P., Borrelli, P., Panagos, P., Ballabio, C., Orgiazzi, A., et al. (2018). Soil Erosion Is Unlikely to Drive a Future Carbon Sink in Europe. *Sci. Adv.* 4, 1–7. doi:10.1126/sciadv.aau3523

Nadeu, E., Berhe, A. A., de Vente, J., and Boix-Fayos, C. (2012). Erosion, Deposition and Replacement of Soil Organic Carbon in Mediterranean Catchments: a Geomorphological, Isotopic and Land Use Change Approach. *Biogeosciences* 9, 1099–1111. doi:10.5194/bg-9-1099-2012

Nitzsche, K. N., Kaiser, M., Premke, K., Gessler, A., Ellerbrock, R. H., Hoffmann, C., et al. (2017). Organic Matter Distribution and Retention along Transects from Hilltop to Kettle Hole within an Agricultural Landscape. *Biogeochemistry* 136, 47–70. doi:10.1007/s10533-017-0380-3

Ostwald, M., and Chen, D. (2006). Land-use Change: Impacts of Climate Variations and Policies Among Small-Scale Farmers in the Loess Plateau, China. *Land Use Policy* 23, 361–371. doi:10.1016/j.landusepol.2005.04.004

Ou, X., Hu, Y., Li, X., Guo, S., and Liu, B. (2021). Advancements and Challenges in Rill Formation, Morphology, Measurement and Modeling. *CATENA* 196, 104932. doi:10.1016/j.catena.2020.104932

Papademetriou, M. K. (2000). "Rice production in the Asia-Pacific Region: Issues and perspectives," in *Bridging the Rice Yield Gap in the Asia-Pacific Region* (Bangkok, Thailand: FAO, UN).

Roser, M., and Ritchie, H. (2019). *"Crop Yields".* Published online at OurWorldInData.org. Retrieved from: https://ourworldindata.org/crop-yields [Online Resource].

Schwanghart, W., Groom, G., Kuhn, N. J., and Heckrath, G. (2013). Flow Network Derivation from a High Resolution DEM in a Low Relief, Agrarian Landscape. *Earth Surf. Process. Landforms* 38, 1576–1586. doi:10.1002/esp.3452

Shen, H., Zheng, F., Wen, L., Han, Y., and Hu, W. (2016). Impacts of Rainfall Intensity and Slope Gradient on Rill Erosion Processes at Loessial Hillslope. *Soil Tillage Res.* 155, 429–436. doi:10.1016/j.still.2015.09.011

Sun, W., Shao, Q., Liu, J., and Zhai, J. (2014). Assessing the Effects of Land Use and Topography on Soil Erosion on the Loess Plateau in China. *CATENA* 121, 151–163. doi:10.1016/j.catena.2014.05.009

Van Oost, K., Cerdan, O., and Quine, T. A. (2009). Accelerated Sediment Fluxes by Water and Tillage Erosion on European Agricultural Land. *Earth Surf. Process. Landforms* 34, 1625–1634. doi:10.1002/esp.1852

Varotto, M., Ferrarese, F., and Pappalardo, S. E. (2019). "Italian Terraced Landscapes: The Shapes and the Trends," in *World Terraced Landscapes: History, Environment, Quality of Life, Environmental History.* Editors M. Varotto, L. Bonardi, and P. Tarolli (Cham: Springer), vol. 9.

Wang, X., Cammeraat, E. L. H., Romeijn, P., and Kalbitz, K. (2014). Soil Organic Carbon Redistribution by Water Erosion - the Role of CO2 Emissions for the Carbon Budget. *PLoS ONE* 9, e96299. doi:10.1371/journal.pone.0096299

Wang, Z., Hu, Y., Wang, R., Guo, S., Du, L., Zhao, M., et al. (2017a). Soil Organic Carbon on the Fragmented Chinese Loess Plateau: Combining Effects of Vegetation Types and Topographic Positions. *Soil Tillage Res.* 174, 1–5. doi:10.1016/j.still.2017.05.005

Wang, Z., Wang, R., Sun, Q., Du, L., Zhao, M., Hu, Y., et al. (2017b). Soil CO 2 Emissions from Different Slope Gradients and Positions in the Semiarid Loess Plateau of China. *Ecol. Eng.* 105, 231–239. doi:10.1016/j.ecoleng.2017.04.050

Wei, W., Chen, D., Wang, L., Daryanto, S., Chen, L., Yu, Y., et al. (2016). Global Synthesis of the Classifications, Distributions, Benefits and Issues of Terracing. *Earth-Science Rev.* 159, 388–403. doi:10.1016/j.earscirev.2016.06.010

Wilken, F., Sommer, M., Van Oost, K., Bens, O., and Fiener, P. (2017). Process-oriented Modelling to Identify Main Drivers of Erosion-Induced Carbon Fluxes. *Soil* 3, 83–94. doi:10.5194/soil-3-83-2017

Yue, Y., Ni, J., Ciais, P., Piao, S., Wang, T., Huang, M., et al. (2016). Lateral Transport of Soil Carbon and Land−atmosphere CO2 Flux Induced by Water Erosion in China. *Proc. Natl. Acad. Sci. USA* 113, 6617–6622. doi:10.1073/pnas.1523358113

Zevenbergen, L. W., and Thorne, C. R. (1987). Quantitative Analysis of Land Surface Topography. *Earth Surf. Process. Landforms* 12, 47–56. doi:10.1002/esp.3290120107